ICAS 2021 SHANGHAI
International Council of the Aeronautical Sciences
32nd Congress of the International Council of the Aeronautical Sciences
September 6-10, 2021
Pudong Shangri-La, Shanghai, China

ENDURANCE ANALYSIS OF BATTERY-POWERED MULTICOPTERS: DERIVATION OF PROPER CUT-OFF VOLTAGE USING DC MOTOR MODEL

Atsushi Satoh[1], Masanao Watanabe[2], Koichi Hozumi[3] & Akira Watanabe[4]

[1]Department of Systems Innovation Engineering, Faculty of Science and Engineering, Iwate University: 4-3-5 Ueda, Morioka, Iwate 020-8550, Japan, Tel & Fax: +81-19-621-6404, E-mail: satsushi@iwate-u.ac.jp
[2]O · T · Techno Research Co., Ltd.: 2-12-4 Osawa, Izumi-ku, Sendai, Miyagi 981-3137, Japan, Tel: +81-22-343–9961, Fax: +81-22-343-9962, E-mail: watanabe@ottr.jp
[3]Japan Aerospace Technology Foundation (JAST): Sendai TM Building, 1-17-26 Ichibancho, Aoba-ku, Sendai, Miyagi 980-0811, Japan, Tel: +81-22-397-6911, Fax: +81-22-397-6889, E-mail: khozumi@nifty.com
[4]4. Japan Aerospace Technology Foundation (JAST), E-mail: akira.watanabe@f-jast.or.jp

Abstract

This work discusses the hover endurance of the battery-powered multicopters from the viewpoint of the battery cut-off condition. In the existing works about the endurance of battery-powered UAVs, the duration for which the battery can supply the required power for steady flight was assumed as flight time. Therefore, the required power based cut-off was assumed in the existing works. On the other hand, the authors derived a cut-off condition according to the *required voltage* for hovering, using a DC motor equivalent circuit model and a battery discharge property model. The authors show that the required voltage based cut-off condition is tighter than the required power based condition, and the former dominates the endurance if typical ESCs are used. The effective capacity depends on the load states which are classified according to the cut-off voltage and discharge property of a battery. The endurance analysis based on the presented results is shown.

Keywords: UAVs, Multicopter, Hover endurance, DC motor equivalent circuit, Discharge cut-off condition

1. Introduction

Nowadays, demands for payload and endurance improvement of multicopters are strongly growing as their application area expands to various industry. To improve the endurance, the use of new power source is attempted (ex. fuel cell[1] or gas-electric system[2]). However the lithium secondary battery powered multicopters are still dominant for the practical use.

The endurance of an electric-powered aircraft basically depends on the required power for steady flight and the effective capacity of a battery. Traub[3, 4, 5] proposed an estimation procedure of the endurance of electric-powered aircraft. In these results, required power for steady level flight is derived from the aerodynamics of the aircraft. An effective capacity of the battery is derived by using Peukert's law[6, 7] (an empirical formula which expresses the reduction in battery capacity for higher discharging rate). The endurance is calculated as the time for which a battery can supply required power. Therefore, a proper estimation of effective capacity is an important issue.

However, the estimates from Peukert's law has some vagueness, because Peukert's law does not depend on a cut-off voltage. Although rated capacity (i.e. the capacity determined from a standard discharge test) is proper to individual batteries, effective capacity varies depending on not only the discharge rate but the cut-off voltage.

One of the purposes of this work is to propose a proper cut-off condition for hovering flight. In [3], the time at which a battery cannot supply the required power is considered as a cut-off condition. However, a voltage based expression of cut-off condition is necessary for estimating effective capacity. Furthermore, typical ESCs (Electric Speed Controllers) do not have voltage step-up function, therefore there are two candidates for the cut-off voltage, namely, required power and require voltage based ones.

In this work, the authors determine the required motor voltage for hovering based on momentum theory and DC motor equivalent circuit model. The authors show that a condition from the required voltage is tighter than another one from the required power, and the former dominates the endurance of the multicopters using standard ESCs. Then, load states in hovering are classified in three cases from the required voltage and D-V property of the battery. The effective capacity is also determined according to the proposed load states. As an application of the above results, evaluation of the hover time and load state of the target multicopter (enRoute PG-560) for several configuration is shown.

2. Required motor voltage for hovering

In this paper, a hovering flight of a multicopter in still air is considered. The electric propulsion system consists of fixed-pitch propellers, blushless DC motors with ESCs (Electric Speed Controller) and lithium polymer (LiPo) batteries is assumed. For simplicity, assume that

Assumption 1.

1. Each propeller is identical and not overlapped.
2. Each propeller is directly driven by a motor.
3. Inductance of a motor is small.

A set of a blushless DC motor with an ESC and a connected propeller is called a “propulsion unit” throughout this paper. An electric propulsion system consists of a LiPo battery[1] and several propulsion units electrically connected in parallel to the battery.
According to the Assumption 1, the loading of one propeller is

$$W_p = \frac{W}{n_r}, \tag{1}$$

where W is take-off weight, n_r is the total number of propellers. Thrust coefficient C_T and torque coefficient C_Q are defined as [9]

$$C_T := \frac{T_p}{\rho \pi R^2 (\omega R)^2}, \tag{2}$$

$$C_Q := \frac{Q_a}{\rho \pi R^3 (\omega R)^2}, \tag{3}$$

where T_p, Q_a are thrust and torque, ρ is air density, R is a propeller radius, ω is an angular velocity of a propeller. Reynolds number effect on C_T, C_Q is small and neglected in this paper. Furthermore, C_T, C_Q are treated as constant throughout this paper because the advance ratio in hovering flight is fixed at zero.
A balance of thrust and loading of the propeller in hovering is

$$T_p = W_p. \tag{4}$$

Adopting the propeller induced velocity derived from simple momentum theory, the work done by the propeller on its inflow per unit time is derived as[9]

$$P_{ih} = W_p \sqrt{\frac{W_p}{2\rho \pi R^2}}. \tag{5}$$

This P_{ih} is the minimum power required for each propulsion unit in hovering. From (2) and (4), angular velocity of a propeller in hovering is derived as

$$\omega_h = \sqrt{\frac{W_p}{C_T \rho \pi R^4}}. \tag{6}$$

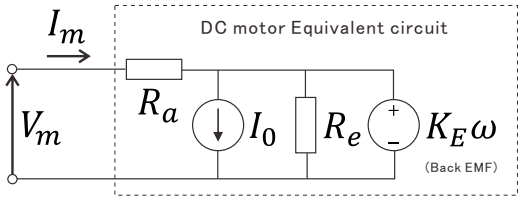

Figure 1 – DC motor equivalent circuit model

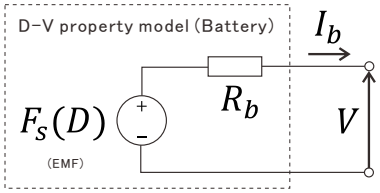

Figure 2 – D-V property model

On the other hand, torque of a DC motor is represented as

$$Q_m = K_T\left(I_m - I_{nl}(\omega)\right) \tag{7}$$

by using DC motor equivalent circuit model[10] (See Figure1), where K_T is torque constant, I_m is motor current, ω is the angular velocity, $I_{nl}(\omega) := I_0 + (K_E/R_e)\omega$ represents no-load current of a motor. In hovering, a balance of propeller and motor torque,

$$Q_a = Q_m, \tag{8}$$

holds. Therefore the motor current in hovering is derived from (3), (6) and (7) as

$$I_{mh} = \frac{C_Q \rho \pi R^5}{K_T}\omega_h^2 + I_{nl}(\omega_h). \tag{9}$$

The first term of the right hand side of (9) is usually much larger than I_{nl} for practical multicopter configurations. Therefore, an approximation of I_{mh} is

$$I_{mh} \simeq \frac{C_Q}{C_T}\frac{R}{K_T}W_p. \tag{10}$$

From the Assumption 1, effect of motor inductance is ignored. Therefore

$$I_m = \frac{V_m - K_E\omega}{R_a} \tag{11}$$

holds. In (11), V_m is motor voltage, K_E is back EMF (Electromotive Force) constant, R_a is the coil resistance of a motor. Note that $K_T = K_E$ for DC motors.
From (11), the required motor voltage to rotate a propeller at ω_h is determined as

$$V_{mh} = R_a I_{mh} + K_E\omega_h \tag{12}$$

Note that V_m in the above discussion is not equal to the battery-side terminal voltage of an ESC. A typical ESC is an inverter without voltage step-up function. Therefore, the ESC applies PWM (Pulse-Width Modulation) to the voltage input to a motor, and steps down the one-cycle-average (OCA) of the input to desired V_m. A voltage applied (in the meaning of OCA) to a motor is determined from the voltage supplied to an ESC and throttle position as

$$V_m^{(\mathrm{OCA})} = V^{(\mathrm{ESC})} \cdot f_{th}(T), \tag{13}$$

where $0 \le T \le 1$ represents normalized throttle position and f_{th} represents throttle characteristic function. The f_{th} is any monotonically increasing function such that

$$0 \le f_{th}(T) \le 1 \text{ for } 0 \le T \le 1, \tag{14}$$

hence $f_{th}(0) = 0$ and $f_{th}(1) = 1$.

[1] A battery is usually made of LiPo cells connected in series/parallel to obtain desired voltage and capacity.

3. Cut-off condition and effective capacity

The discharge capacity of a battery is defined as the quantity of the extracted electric charge in constant rate discharge[11]. In what follows, the authors simply use the term “capacity” as the meaning of discharge capacity. The end of discharge is when the battery’s terminal voltage drops to some cut-off voltage. Because of battery internal resistance, the higher discharge rate is, the lower terminal voltage is, and it causes the reduction in battery capacity. Therefore, an effective capacity depends on the condition of discharge (i.e. discharge current and cut-off voltage).
IEC 61960-3 standard[11] defines the condition and procedure to determine “rated capacity” of the lithium secondary battery. In the definition, discharge rate is specified as $0.2C$ [2], and the cut-off voltage is what should be specified by the battery manufacturer (usually about 2.5 [V] per cell).
The terminal voltage during discharge is lower than open circuit voltage (OCV) because of the internal voltage drop caused by battery impedance. The propulsion system in hovering requires constant power. As the terminal voltage gradually drops by discharging, throttle control is required to increase battery current and maintain constant power.
In this work, simplified battery model (let us call “D-V property model”) only considering internal resistance component (Figure2) is used under the assumption of the rate of change of discharge current is not high in hovering.

$$V(D,I) = F_s(D) - R_b I \tag{15}$$

In (15), V is battery terminal voltage, I is discharge current, $0 \leq D \leq 1$ is the depth of discharge (DoD). $D(t) := I \cdot t / Q_{rat}$ for discharge time t, where Q_{rat} represents rated capacity. Therefore $D = 0$ means full charge and $D = 1$ means full discharge. F_s is OCV and R_b is internal resistance. Let us assume that

Assumption 2. $F_s(D)$ is monotonously decreasing and $F_s(D) > 0 \quad (0 \leq D \leq 1)$.

Therefore the maximum of the OCV is $F_s(0) =: V_{full}$. From (15), an OCV-based cut-off voltage V_{end} is defined as

$$V_{end} := V_{end}^{rat} + R_b I_{0.2C}, \tag{16}$$

where V_{end}^{rat} is the terminal voltage based cut-off for the discharge test to determine rated capacity. $I_{0.2C}$ represents the discharge current which corresponds to $0.2C$ for each cell. Furthermore, the terminal voltage based cut-off for a discharge current I_b is defined as $V_{end}^{TV}(I_b) := V_{end} - R_b I_b$ from (15). For simplicity, let us make an assumption for ESC and battery.

Assumption 3.

1. The current between a battery and an ESC is not changed by the switching operation in the ESC.
2. The voltage drop because of the wire resistance between a battery and an ESC is ignored. The power loss by switching operation in the ESC is also ignored.
3. The temperature of a battery does not change in hovering. At the start of hovering (or equivalently, discharging), the battery is fully charged and in steady state.

Firstly, consider a hovering condition from the viewpoint of required power. For each propulsion unit, the required electric power in hovering is calculated as $P_{eh} := V_{mh} I_{mh}$. A balance of the power consumed by the propulsion system and supplied by the battery is

$$n_r P_{eh} = V(D, I_b) I_b = F_s(D) I_b - R_b I_b^2, \tag{17}$$

where I_b is battery current.
If a multicopter can hover, the equation (17) must have at least one real I_b as a solution. Therefore the power-based condition for the hovering at the initial time (Remember that $D = 0$ at the initial time) is derived from the discriminant of (17) as

$$F_s(0) \geq 2\sqrt{R_b n_r P_{eh}} = 2\sqrt{R_b I_h \cdot V_{mh}} =: V_{sp}, \tag{18}$$

[2] “C” means “Capacity rate”. The capacity rate is defined as the ratio of discharge current [A] to rated capacity [Ah].

where the total of the motor current in hovering is defined as $I_h := n_r I_{mh}$.
We can assume input impedance of an ESC is higher than R_b. Therefore

$$I_b(D) = \frac{F_s(D) - \sqrt{F_s^2(D) - V_{sp}^2}}{2R_b} \tag{19}$$

from (17).
Secondly, consider another hovering condition from the viewpoint of required voltage. For a fixed V_{mh}, the minimum voltage should be supplied to the ESC is also V_{mh}, from (13) and (14) with $T = 1$, then $I_b = I_h$ from the balance of power.
Therefore, if the multicopter can hover, the initial terminal voltage must exceed the required motor voltage for hovering. From the Assumption 2, a voltage-based condition for the hovering at the initial time is derived as

$$V(0, I_h) > V_{mh} \Leftrightarrow F_s(0) > V_{mh} + R_b I_h =: V_{sh}. \tag{20}$$

From the inequality of arithmetic and geometric means and considering $V_{mh} \gg R_b I_h$ for practical working conditions,

$$V_{sh} > V_{sp} \tag{21}$$

holds. Therefore an essential voltage condition which determines hover duration is (20), rather than (18).
From (6), (10) and (12), V_{sh} can be described as

$$V_{sh}(W) = \left(\frac{R_a}{n_r} + R_b\right) \cdot \frac{C_Q R}{C_T K_E} \cdot W + K_E \sqrt{\frac{W}{n_r C_T \rho \pi R^4}}. \tag{22}$$

Let us call V_{sh} in (22) "voltage-required" in hovering. We can see V_{sh} is monotonously increasing for take-off weight W. Note that $T_h := n_r T_p(\omega_h)$, $C_Q R / C_T K_E = I_h / T_h = I_h / W =: b_{mh}$ is the specific motor current in hovering. From (22), V_{sh} have a minimum with respect to K_E.

$$\min_{K_E}(V_{sh}) = 2\left\{\sqrt{\frac{W}{n_r C_T \rho \pi R^4}}\left(\frac{R_a}{n_r} + R_b\right) \cdot \frac{C_Q R}{C_T} \cdot W\right\}^{\frac{1}{2}} = 2\omega_h K_E^{min}, \tag{23}$$

for

$$K_E^{min} = \left\{\sqrt{\frac{n_r C_T \rho \pi R^4}{W}}\left(\frac{R_a}{n_r} + R_b\right) \cdot \frac{C_Q R}{C_T} \cdot W\right\}^{\frac{1}{2}}. \tag{24}$$

The inequality (20) implies there exists some $t_h > 0$ such that $F_s(D(t)) \geq V_{sh}$ for $0 \leq t \leq t_h$. Therefore, the hover duration is interpreted as the duration for which the F_s ("voltage-available" in the sense of OCV) exceeds the V_{sh} (voltage-required).
From the viewpoint of the battery capacity, V_{sh} in (22) is considered as an OCV based proper cut-off voltage for a certain load state defined in the following. The load states of the propulsion system in hovering are classified in three cases shown in Figure3.

Admissible load ($V_{end} < V_{sh} < V_{full}$) At the end of hovering, $T = 1$ and $V = V_{mh}$. This means there is no room for increasing throttle position to keep hovering. Therefore, the cut-off voltage is V_{sh} in (22) and the effective capacity is less than Q_{rat}.

Rated load ($V_{sh} \leq V_{end}$) At the end of hovering, $T \leq 1$ and $V = V_{end}^{TV}(I_b(1))(\geq V_{mh})$. This means the battery is fully discharged until the rated capacity is achieved. Therefore, the cut-off voltage is V_{end} in (16) and the effective capacity is equal to Q_{rat}[3].

Overload ($V_{full} \leq V_{sh}$) Impossible to hover.

[3]Note that the effective capacity does not exceeds Q_{rat} even if $V_{sh} < V_{end}$

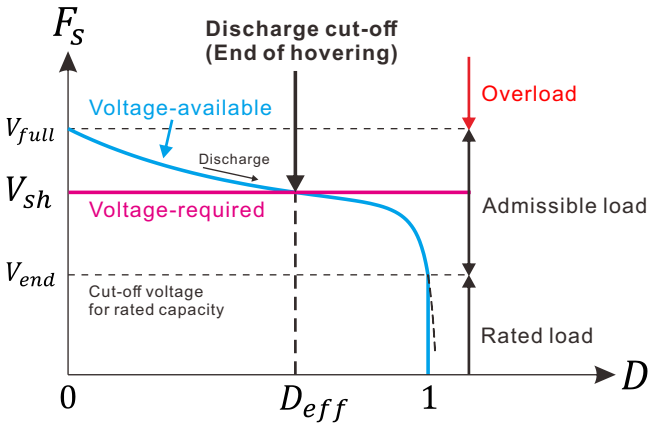

Figure 3 – Load states

From the above discussion, the effective capacity in hovering is described as

$$Q_{eff}(V_{sh}) = D_{eff}(V_{sh})Q_{rat}. \tag{25}$$

The D_{eff} is the specific effective capacity of the battery or similar to Coulombic efficiency (CE) in battery analysis. Using the D-V property model in (15),

$$D_{eff} = \begin{cases} F_s^{-1}(V_{sh}) & (V_{end} < V_{sh} < V_{full}) \\ 1 & (V_{sh} \le V_{end}) \end{cases}, \tag{26}$$

where F_s^{-1} $(0 \le F_s^{-1} \le 1)$ is the inverse function of F_s.

4. Hover endurance

Consider discharging in constant current I_b for dt. The capacity $dQ = I_b dt$, and $t = \int dt = \int (1/I_b) dQ$. From (25), the hover time t_h for given V_{sh} is represented as

$$t_h = \int_0^{D_{eff}} \frac{Q_{rat}}{I_b(D)} dD. \tag{27}$$

From the definition of the admissible and rated load,a lower bound of t_h is obtained as

$$t_h \ge D_{eff} \cdot \frac{Q_{rat}}{W} \cdot b_{mh}^{-1} \cdot \frac{I_h}{I_b(1)}, \tag{28}$$

where Q_{rat}/W is capacity-weight ratio. Note that $I_h/I_b(1) \ge 1$ ($I_h/I_b(1) = 1$ for the admissible load). If we adopt $(I_b(0) + I_b(D_{eff}))/2$ as a representative battery current, the next approximation is obtained.

$$t_h \simeq D_{eff} \frac{2Q_{rat}}{I_b(0) + I_b(D_{eff})} =: \tilde{t}_h. \tag{29}$$

5. Endurance analysis of multicopter

5.1 Measurement of propulsion system parameters

The target aircraft of the endurance analysis is enRoute PG-560 quadcopter (Figure4). Parameters of the propulsion system are shown in Table1.

The authors developed a test bench for the measurement of the characteristics of electric propulsion systems (Figure5). This equipment can measure the static thrust, torque, rotational speed of the propeller, and the consumed electric power by the propulsion unit.

The normalized throttle positions for the measurement are

$$T \in \{0.2, 0.3, 0.4, 0.5, 0.6, 0.7, 0.8, 0.9\}. \tag{30}$$

Figure 4 – enRoute PG-560 quadcopter

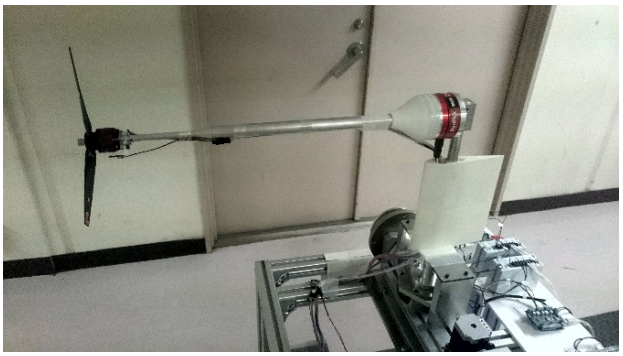

Figure 5 – Test bench for electric propulsion system

The pulsewidth of PWM signal to control an ESC is determined as $(1.0+T)$[ms]. The rotational speed of the propeller was measured by a Hall sensor (Melexis US1881). Propeller thrust and torque was measured by a 6-axis force torque sensor (WACOH-TECH WEF-6A200-4-RC5). Electric power consumption at the inlet of an ESC is measured by using a current shunt and a power monitor (Texas Instruments INA226). A switching DC power supply (TEXIO PSW-720L30) is used as the power source of the propulsion unit.
For the propulsion system of PG-560, the rotational speed of the propeller is almost in proportion to the throttle position. A least-square fitting model is ω[rad/s] $= 670.77T - 7.1314\ (0 \leq T \leq 1)$. Measured C_T and C_Q are shown in Figure6. P_e, $P_a - P_e$ (power loss) and $\eta := P_a/P_e$ (motor efficiency) are shown in Figure7. K_E, R_a are estimated from no-load rotation tests and shown in Table2. Calculated KV rating[4] of the motor is 333 [rpm/V] This result is very similar to the value from the specification in Table1 $(330$ [rpm/V]).

5.2 Modeling of D-V property

An OCV property of a battery is modeled by using "Nernst model"[8] in this work. According to this model, the OCV property of a cell is represented as

$$f_{ocv}(D) \quad = \quad E^0 + a\ln(1-D+\varepsilon_1) + b\ln(D+\varepsilon_2) + c(1-D+\varepsilon_1)^{-1} + d(1-D+\varepsilon_1), \tag{31}$$

where E^0 is standard electrode potential. The parameters (a,b,c,d) are the characteristics parameters of a cell. The adjustment parameters $\varepsilon_1, \varepsilon_2 > 0$ are introduced to keep f_{ocv} finite at $D = 0, 1$.
A battery is usually made of several cells connected in series/parallel. Furthermore, batteries may be connected each other on board. Therefore, assume the assembly of all cells on board as a virtual large battery.

Assumption 4.

[4] $KV = (K_E[\text{V/rpm}])^{-1}$.

Table 1 – Propulsion system specifications (enRoute PG-560)

Propeller (CFRP)	enRoute EXC044	Diameter 15[in] (=381[mm]), Pitch 5.5[in]
Brushless DC motor	enRoute Zion 4631-330KV	KV 330[rpm/V], 24 Poles
ESC	enRoute Zion M40A	max current 40[A], LiPo cells 2∼6
Battery (LiPo)	enRoute Zion 99Wh	6 Cells, Weight 0.797[kg]

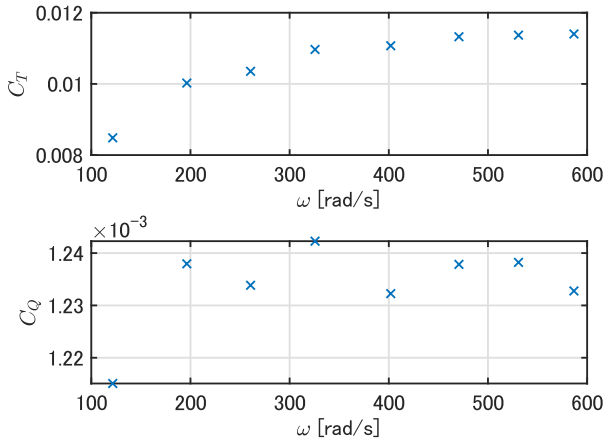

Figure 6 – C_T and C_Q (enRoute EXC044 propeller)

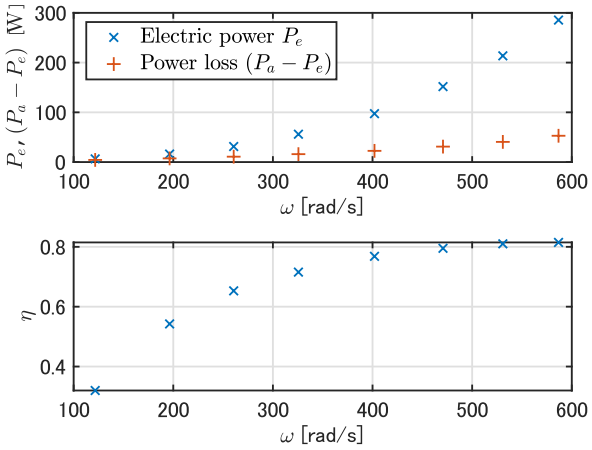

Figure 7 – P_e, $(P_a - P_e)$ and η (enRoute Zion 4631-330KV motor with Zion M40A ESC)

1. Characteristics of all cells are identical.
2. The total number of cells is $n_s \times n_p$, where n_s, n_p are the number of cells connected in series or parallel, respectively.

Then the OCV of the virtual battery is described as $F_s(D) = n_s f_{ocv}(D)$. The internal resistance R_b of the virtual battery is described as

$$R_b = \frac{n_s}{n_p} R_{cell}, \tag{32}$$

where R_{cell} is the internal resistance of a cell.
The results of the constant current discharge tests of enRoute Zion 99Wh LiPo battery is shown on Figure8. R_{cell} is estimated from the averaged terminal voltage in $0.4 \leq D \leq 0.8$ for each discharge test. The parameters in (31) are determined by using "fit" function from MATLAB R2018 Curve Fitting Toolbox. The fitted parameters are shown in Table3. A determined D-V property model is shown in Figure9. Note that early responses (i.e. $D \simeq 0$) in discharge were excluded for the parameter fitting (shown in Figure9 by "x" marker).

5.3 Endurance analysis

The empty weight[5] W_{emp} of PG-560 is shown in Table2. A payload is defined as $W_{pay} := W - W_{emp}$.
In this section, hovering time is numerically evaluated using the measured parameters and D-V property model of the target multicopter. The parameters for the parametric study are take-off weight W

[5]The empty weight is the weight of the multicopter without including batteries and application payloads (ex. a movie camera).

Table 2 – Measured parameters

Body (enRoute PG-560)	n_r	4
	W_{emp} [N] (empty weight)	19.6
Propeller (enRoute EXC044)	R [m]	0.19
	ρ [kg/m^3]	1.19
	C_T (Average for $121.6 \leq \omega$[rad/s] ≤ 586.7)	0.0106
	C_Q (Average for $121.6 \leq \omega$[rad/s] ≤ 586.7)	0.00123
Brushless DC Motor (enRoute Zion 4631-330KV)	K_E [V $\cdot$ s/rad]	0.0287
	R_a [Ω]	0.20

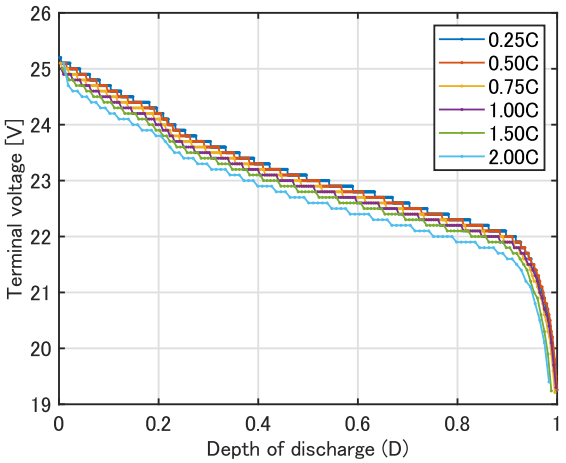

Figure 8 – Terminal voltage in constant current discharge (enRoute Zion 99Wh battery, 22.5 ± 1[°C])

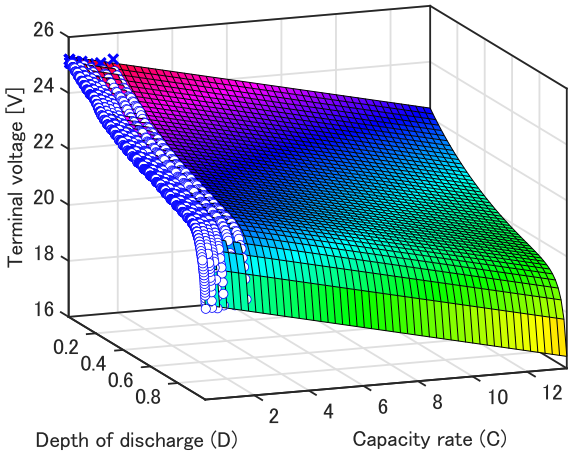

Figure 9 – D-V property model (enRoute Zion 99Wh battery)

and payload-battery weight ratio $\lambda_{pay} := W_{batt}/W_{pay}$. The rated capacity for this study is assumed to be continuous valued, namely, not constrained to the integer multiple of the cell capacity of the test battery (Q_{cell} in Table2). Throughout the study, $n_s = 6$ (fixed) and $n_p = Q_{rat}/Q_{cell}$. The parameter combination for the study is

$$(W, \lambda_{pay}) \quad \in \quad \{W_{emp} + 2(n-1)[\mathrm{N}], n = 1, \ldots, 30\} \times \{0.1m, m = 1, \ldots, 10\}. \tag{33}$$

Figure10 shows the t_h in (27). The maximum hover time (36.7 [min]) was obtained for $(W, \lambda_{pay}) = (5.67$ [kgf]$, 1)$. Note that the areas colored yellow in Figure10-12 represent non-practical configurations because of poor weight-thrust ratio ($T_h^{max}/W < 1.3$).
From Figure11, we can see the large area of the practical configurations corresponds to rated load. The target multicopter is designed for the flight with $1 \sim 2$ batteries (Zion 99Wh). These configurations are represented by two magenta curves in Figure11. Most part of these lines are included in the rated load area.
Figure12 shows the $\tilde{t}_h$ in (29). Comparing Figure10 and 12, although an approximation error becomes larger for small W, $\tilde{t}_h$ is useful to obtain rough estimates. For a large scale parameter study, a piecewise linear approximation of F_s^{-1} is useful for fast calculation.

6. Conclusions

In this work, the hover endurance of the battery-powered multicopters is discussed from the viewpoint of the battery cut-off condition. Endurance of the electric-powered aircraft is basically depends on required power for steady flight and effective capacity of a battery. In the pioneering works by Traub[3, 4, 5], the use of the discharge time estimated by using Peukert's law[6, 7] was proposed. However, this estimate has a vagueness because Peukert's law does not depend on cut-off voltage which is

Table 3 – Parameters in D-V property model (enRoute Zion 99Wh)

(n_s, n_p)	(6, 0)
$(\varepsilon_1, \varepsilon_2)$	(0.05, 0.5)
(a, b, c, d)	(-0.2257, -0.6983, -0.0477, -0.0022)
E^0 [V]	3.8
R_{cell} [Ω]	0.0083

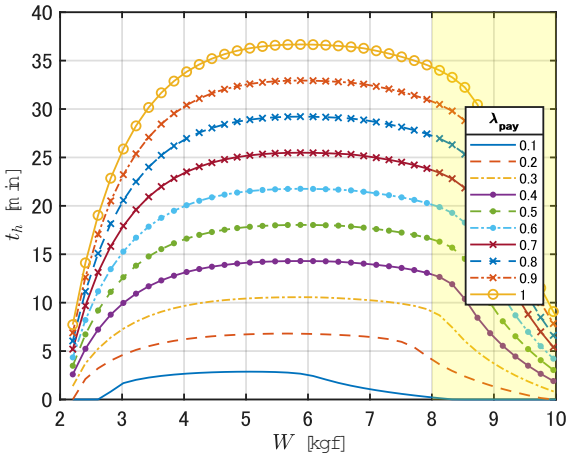

Figure 10 – Hover endurance t_h

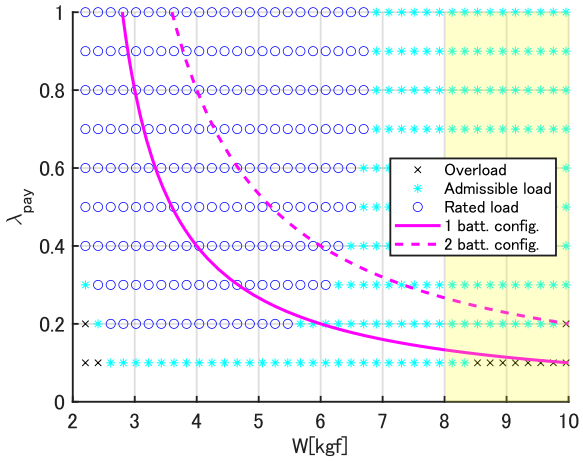

Figure 11 – Load states for (W, λ_{pay})

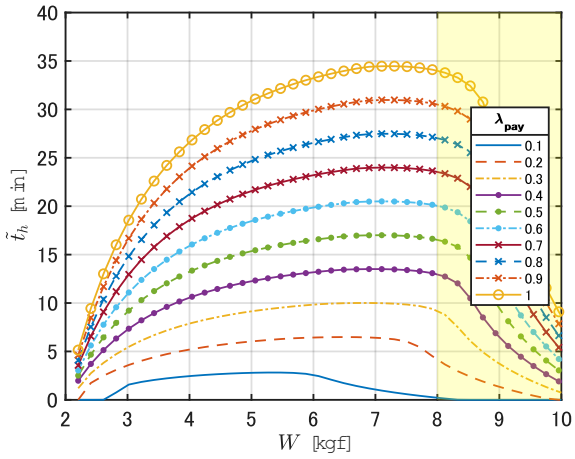

Figure 12 – Approximated hover endurance $\tilde{t}_h$

an essential information to determine the discharge capacity of a battery. Furthermore, the cut-off voltage varies depending on take-off weight.

To elucidate proper cut-off conditions for hovering flight, the authors determined the required motor voltage in hovering, using DC motor equivalent circuit model. After that, the condition from the required voltage in (20) is proved to be tighter than that from the required power in (18) when typical ESCs that do not have voltage step-up function are used.

The hover duration is interpreted as the duration for which the "voltage-available" F_s exceeds the "voltage-required" V_{sh}. The authors introduced the classification of load states of the propulsion system by using F_s and V_{sh}, and made clear how the effective capacity depends on the load status. Hovering time was defined in a similar manner for engine-powered aircraft, by using specific effective capacity D_{eff}, rated capacity Q_{rat} and battery current (or electric charge consumption rate) I_b.

As an application of the presented results, a parametric study was conducted to evaluate the hover time of the target multicopter (enRoute PG-560) for several combination of the take-off weight and payload-battery weight ratio.

Acknowledgements

The authors would like to thank M. Kikuchi, technical staff member of Iwate university for developing research equipment. This work is partially supported by the discretionary expense of the dean of the faculty of science and engineering, Iwate university, and Soft-Path Engineering Research Center

(SPERC), faculty of science and engineering, Iwate university.

7. Contact Author Email Address

mailto: satsushi@iwate-u.ac.jp

8. Copyright Statement

References

[1] Hycopter Hydrogen-Electric UAV, `https://www.airforce-technology.com/projects/hycopter-hydrogen-electric-uav/`, Accessed on 31st May 2021.

[2] QL1600 Hybrid System Drone, `https://www.walkera.com/index.php/Goods/info/id/82.html`, Accessed on 31st May 2021.

[3] L. W. Traub Range and Endurance Estimates for Battery-Powered Aircraft. *J. Aircraft*, Vol. 48, No. 2, pp 703-707, 2011.

[4] L. W. Traub Validation of Endurance Estimates for Battery Powered UAVs. *Aeronaut. J.*, Vol. 117, No. 1197, pp 1-12, Nov. 2013.

[5] L. W. Traub Optimal Battery Weight Fraction for Maximum Aircraft Range and Endurance. *J. Aircraft*, Vol. 53, No. 4, pp. 1177-1179, 2016.

[6] W. Peukert Über die Abhängigkeit der Kapazität von der Entladestromstärke bei Bleiakkumulatoren. *Elektrotechnische Z.*, Vol. 20, pp 287-288, 1897. (In German)

[7] C. Nebl et al. Discharge Capacity of Energy Storages as a Function of the Discharge Current –Expanding Peukert's equation. *Int. J. Electrochem. Sc.*, Vol. 12, pp. 4940-4957, 2017.

[8] G. L. Plett Extended Kalman filtering for battery management systems of LiPB-based HEV battery packs Part 2. Modeling and identification, *J. Pow. Sources*, Vol. 34, pp. 262-276, 2004.

[9] B. W. McCormick. *Aerodynamics, aeronautics, and flight mechanics*. John Wiley & Sons, 1979.

[10] T. Kenjo. *Electric motors and their controls: An introduction*. Oxford University Press, 1991.

[11] Secondary cells and batteries containing alkaline or other non-acid electrolytes - Secondary lithium cells and batteries for portable applications - Part 3: Prismatic and cylindrical lithium secondary cells and batteries made from them, *IEC 61960-3:2017*, 2017.